THREE-DIMENSIONAL HYDRODYNAMIC MODEL COUPLED WITH DEPTH AVERAGED TWO-DIMENSIONAL MODEL : CASE OF THE MEDJERDA-CAP-BON WATER INTAKE.

Zouhaier HAFSIA[(1)] et Khlifa MAALEL[(2)]

[(1) et (2)] Ecole Nationale d'Ingénieurs de Tunis. Laboratoire d'Hydraulique.

B.P. 37 - Le Belvédère, 1002, Tunis, Tunisie.

E-mail : [(1)] Zouhaier.Hafsia@enit.rnu.tn [(2)] Khlifa.Maalel@enit.rnu.tn

Date : 04/02/2000

Hardware : Sun Sparc Station 5

PHOENICS version : 2.10

ABSTRACT

The purpose of this study is to modify the currents structures at the entry of Medjerda-Cap-Bon water intake, alimented from the Laroussia dam reservoir, in order to reduce the upwelling of bottom currents toward its conveyance channel. The currents structures is identified by visualization on an hydraulic model (horizontal scale 1/100 and vertical scale 1/25) and by numerical simulations using three-dimensional hydrodynamic model (3-D) coupled with the results of depth-averaged two-dimensional hydrodynamic model (2-DH). The continuity and Reynolds equations describing the hydrodynamic are written in curvilinear coordinate system. For the 3-D hydrodynamic model, the grid is generated in BFC "Body-Fitted Coordinates" while a multi-block grid is used for the 2-DH model. The visualized bottom currents shows an inversion of secondary currents direction under the effect of an approach-channel. This inversion implies a reduction of the bottom currents upwelling and by following the entrance of mud particles in the MCB channel. These results are confirmed by the numerical simulations corresponding to the hydraulic model scale and field scale.

TABLE OF CONTENTS

1- PROBLEM DESCRIPTION

The Laroussia dam is located on the low valley of the Medjerda stream. Its normal level is fixed to 37.50 m. This dam assure the water demand of three water intakes (Figure 1) : the hydroelectric power station intake (C), the Great-Channel (GC) and the Medjerda-Cap-Bon (MCB) deriving respectively a maximum discharge of 50 m^3/s, 13 m^3/s and 16 m^3/s. The GC and MCB intakes allow to satisfy irrigation and drinking water demand. Since 1989, an islet of mud deposits has been observed in front of the MCB intake and important quantities of deposits have been recorded along its channel conveyance.

To identify and thereafter analyze the effects of currents structures in the observed mud deposits, visualization tests on an hydraulic model with fixed bed have been realized. This approach allows to overcome the difficulties of the interpretation of hydraulic model results with movable bed (Bouvard, 1984). To overcome the costs and delays of constructing and runing of hydraulic models, often very large, sevral computational fluid dynamics (CFD) code have been used as an aid tool for the design of waterworks (spillway, energy dissipation basin, intake structures) and to verify the efficiency of the proposed sediment control device (Atkinson, 1988; Higgs, 1997). However, the numerical predetermination of three-dimensional currents structures in the large systems requires very important time computation. To reduce costs of computations, three-dimensional hydrodynamic models (3-D) are applied on a less extended zone than the global domain and where the 3-D phenomena are important. Results of these models are then coupled, through boundary conditions, to those of a mono or two-dimensional model (Wang, 1991).

We present in this study an approach that consists in coupling three-dimensional hydrodynamic model in the Laroussia dam reservoir with results of depth-averaged two-dimensional model. The simulated results, validated by visualization tests on hydraulic model, permitted to confirm the advantage of the proposed approach-channel on the field scale (the prototype).

2- DESCREPTION OF THE HYDRAULIC MODEL AND OF THE BASIC EQUATIONS OF THE MATHEMATICAL MODEL

2.1- Hydraulic model

It is a fixed bed model built on a rectangular experimental channel having 12.18 m long, 2.00 m wide and 0.6 m depth. In a turbulent free surface flows, it is essential to

assure the similarity of the volume forces (inertia and gravity) and surface forces (viscous and turbulent shear stress). Therefore, it is necessary to conserve the same Froude number and Reynolds number in the hydraulic model and on the field scale. Assuming that the liquid is the same on the model and the prototype, it is impossible to satisfy these two criterias. For a given relative roughness, it is suffisent to conserve the same flow regime on the model and the prototype, often turbulent rough (Henderson, 1966). This implies that the Reynolds number is at least equal to 1400 according to Henderson, and that the Froude similarity is also satisfied. A distorded hydraulic model is adopted to take into account these limitations and the constraints imposed by the experimental channel. This distortion is defined as the ratio of the vertical scale (h_r = 1/25) to the horizontal scale (L_r = 1/100) taken equal to $\Delta = h_r/L_r = 4$. Visualization tests concerned the normal operating flow conditions : the three Laroussia dam gates are closed and reservoir level is maintained fixed to its normal level, 37.50 m. The derived discharge through each water intake is taken equal to the maximal discharge.

2.2- Mathematical model

2.2.1- Basic equations

Assuming that the flow regime is steady and the liquid is incompressible and newtonien, we can write the general and conservative form of the balance equations in the curvilinear coordinate system (ξ, η, ζ) as (Smith and al., 1993) :

$$\underbrace{\frac{\partial}{\partial\xi}(\rho\, U\phi)+\frac{\partial}{\partial\eta}(\rho\, V\phi)+\frac{\partial}{\partial\zeta}(\rho\, W\phi)}_{(a)}=\frac{\partial}{\partial\xi}\left(\frac{\Gamma_\phi}{J}(q_{11}\,\phi_\xi+q_{12}\,\phi_\eta+q_{13}\,\phi_\zeta)\right)+\frac{\partial}{\partial\eta}\left(\frac{\Gamma_\phi}{J}(q_{21}\,\phi_\xi+q_{22}\,\phi_\eta+q_{23}\,\phi_\zeta)\right)+\underbrace{\frac{\partial}{\partial\zeta}\left(\frac{\Gamma_\phi}{J}(q_{31}\,\phi_\xi+q_{32}\,\phi_\eta+q_{33}\,\phi_\zeta)\right)}_{(b)}+\underbrace{J\,S_\phi}_{(c)} \quad (1)$$

with,

ρ : liquid density

$J=\dfrac{\partial(x,y,z)}{\partial(\xi,\eta,\zeta)}$: Jacobian of the transformation from the Cartesian coordinate system (x, y, z) to the curvilinear coordinate system (ξ, η, ζ).

$$J=(y_\eta z_\zeta-y_\zeta z_\eta)x_\xi-(x_\eta z_\zeta-x_\zeta z_\eta)y_\xi+(x_\eta y_\zeta-x_\zeta y_\eta)z_\xi \quad (2)$$

U, V and W are the contravariant velocity components defined by :

$$U = J\left(u\xi_x + v\xi_y + w\xi_z\right),\ V = J\left(u\eta_x + v\eta_y + w\eta_z\right) \text{ et } W = J\left(u\zeta_x + v\zeta_y + w\zeta_z\right) \quad (3)$$

ϕ : transport variable (the velocity components in momentum transport equation).

The metric coefficients in the transport equation (1) is determined by the following expressions :

$$q_{11} = \left(y_\eta z_\zeta - y_\zeta z_\eta\right)^2 + (x_\eta z_\zeta - x_\zeta z_\eta)^2 + (x_\eta y_\zeta - x_\zeta y_\eta)^2 \quad (4\text{-a})$$

$$q_{22} = (y_\zeta z_\xi - y_\xi z_\zeta)^2 + (x_\zeta z_\xi - x_\xi z_\zeta)^2 + (x_\zeta y_\xi - x_\xi y_\zeta)^2 \quad (4\text{-b})$$

$$q_{33} = (y_\xi z_\eta - y_\eta z_\xi)^2 + (x_\xi z_\eta - x_\eta z_\xi)^2 + (x_\xi y_\eta - x_\eta y_\xi)^2 \quad (4\text{-c})$$

$$q_{12} = q_{21} = (y_\eta z_\zeta - y_\zeta z_\eta)(y_\zeta z_\xi - y_\xi z_\zeta) + (x_\eta z_\zeta - x_\zeta z_\eta)(x_\zeta z_\xi - x_\xi z_\zeta) + (x_\eta y_\zeta - x_\zeta y_\eta)(x_\zeta y_\xi - x_\xi y_\zeta) \quad (4\text{-d})$$

$$q_{13} = q_{31} = (y_\eta z_\zeta - y_\zeta z_\eta)(y_\xi z_\eta - y_\eta z_\xi) + (x_\eta z_\zeta - x_\zeta z_\eta)(x_\xi z_\eta - x_\eta z_\xi) + (x_\eta y_\zeta - x_\zeta y_\eta)(x_\xi y_\eta - x_\eta y_\xi) \quad (4\text{-e})$$

$$q_{23} = q_{32} = (y_\zeta z_\xi - y_\xi z_\zeta)(y_\xi z_\eta - y_\eta z_\xi) + (x_\zeta z_\xi - x_\xi z_\zeta)(x_\xi z_\eta - x_\eta z_\xi) + (x_\zeta y_\xi - x_\xi y_\zeta)(x_\xi y_\eta - x_\eta y_\xi) \quad (4\text{-f})$$

where the lower indices indicate partial derivatives.

Equation (1) can be interpreted as a balance between non-linear convection terms (a), a diffusion term (b) and a source term (c). The pressure gradients are the only sources terms considered in momentum equations :

$$S_u = -\frac{\partial P}{\partial x} = -\left(\xi_x P_\xi + \eta_x P_\eta + \zeta_x P_\zeta\right);\ S_v = -\frac{\partial P}{\partial y} = -\left(\xi_y P_\xi + \eta_y P_\eta + \zeta_y P_\zeta\right) \text{ et } S_w = -\frac{\partial P}{\partial w} = -\left(\xi_z P_\xi + \eta_z P_\eta + \zeta_z P_\zeta\right) \quad (5)$$

The continuity equation is deduced from the equation (1) by taking ϕ = 1 and assuming no term source. For the turbulent flows, and by applying the Reynolds decomposition, the non-linearity of the convection term (a) introduces additional terms called Reynolds stress. The hypothesis usually used in turbulence models is based on the turbulent viscosity concept conferring to the Reynolds stress a diffusif character from a gradient law and hence linear (Schiestel, 1993). The diffusion coefficient of the equation (1) is therefore writen as :

$$\Gamma_\phi = \mu_t + \mu \quad (6)$$

According to the number of transport equations considered to determine the turbulent viscosity field, different types of turbulence models are distingueshed : with zero,

one or two transport equations (Schiestel, 1993). In the case of the Laroussia dam reservoir, we adopted a constant turbulent viscosity model. This implies that the turbulence is dissipated where it is produced. This model allowed to overcome the difficulty to control the non orthogonal grid distribution close to the wall; which is essential to determine the near wall variables in the k-ε turbulence model. The value of turbulent viscosity is determined by the comparaison between the visualised and simulated currents and is equal to, $\nu_t = 10^{-5}$ m^2/s on hydraulic model scale ($\nu_t = 2.5\ 10^{-2}$ m^2/s on field scale).

Assuming that the flow depth is neligeable compared to the width, which is the case of the MCB intake convergent, the integration of the equation (1) over the flow depth provides the depth-avereged hydrodynamic equation in the (ξ, η) plan. This model is described by the following transport equation (Jian and McCorquodale, 1997):

$$\frac{\partial}{\partial\xi}(\rho H U\phi)+\frac{\partial}{\partial\eta}(\rho H V\phi)=\frac{\partial}{\partial\xi}\left(\frac{H\Gamma_\phi}{J}(q_{11}\,\phi_\xi-q_{12}\,\phi_\eta)\right)+\frac{\partial}{\partial\eta}\left(\frac{H\Gamma_\phi}{J}(-q_{12}\,\phi_\xi+q_{22}\,\phi_\eta)\right)+J\,S_\phi(\xi,\eta) \tag{7}$$

where H is the flow depth,

The coefficient q_{ij} (i and j =1,2) in the (ξ, η) plan are determined from equations (4-a to 4-f) considering that the z-axis is invariant. Source terms of equation (7) introduce bed shear stress τ_{bi}, in addition to pressure gradients :

$$S_u=-\frac{\partial}{\partial x}(H\,P)=-\left(\xi_x(H\,P)_\xi+\eta_x(H\,P)_\eta\right)-\tau_{bx} \tag{8-a}$$

$$S_v=-\frac{\partial P}{\partial y}(H\,P)=-\left(\xi_y(H\,P)_\xi+\eta_y(H\,P)_\eta\right)-\tau_{by} \tag{8-b}$$

with:

$$\tau_{bx}=\frac{\rho\,g\,u\sqrt{u^2+v^2}}{H\,C^2}\qquad\text{et}\qquad\tau_{by}=\frac{\rho\,g\,v\sqrt{u^2+v^2}}{H\,C^2} \tag{8-c}$$

where, g : gravity acceleration,

C: Chezy friction coefficient expressed in terms of the Manning-Strickler friction coefficient, K, by :

$$C=K\,R^{1/6}\ ;\ \text{and}\ \ K=\frac{8.25\sqrt{g}}{d_{90}^{1/16}} \tag{9}$$

Whith R is the hydraulic radius; d_{90} is the diameter sediment particle of which 90% of weight is finer.

2.2.2- Boundary conditions

Boudary conditions of the three-dimensional hydrodynamic model given by equation (1), concern the definition of inflow, outflow, the rigid wall, free surface conditions and blockages. At the inlet, longitudinal velocity component is assumed to have a uniform distribution determined by the corresponding inlet discharge (for discharge ratio equal to 1/12500, the discharge on the hydraulic model scale is: Q = 16/12500 = 1.3 l/s). At the MCB intake exit, the horizontal velocity components are fixed from results of the depth-averaged two-dimensional hydrodynamic model described by equation (7), (Figures 2 and 3). These imposed velocity components permitted to account for the effect of the MCB intake convergent on the kinematic field of the Laroussia dam reservoir. And therefore, the study domain of the three-dimensional hydrodynamic model was limited to the Laroussia reservoir only. We adopted the classical conditions with logarithmic profile of the streamwise velocity as conditions on the bottom and lateral walls of the reservoir. The shear velocity is computed based on avareged Manning-Strickler coefficient fixed to: K = 33 $m^{1/3}$/s. The free surface is treated as a rigid wall without friction. Finally, we note that the Laroussia dam gates and their piers (PVD, PVC and PVG) are considered as a blockages.

2.2.3- Treatment of pressure-velocity coupling

In PHOENICS code, the transport equations is discretized by the finite volume method. A cell center grid arrangement using covariant velocity components is adopted in the 2-DH hydrodynamic model while in the 3-D hydrodynamic model, a staggered grid arrangement is used. In this case, scalar variables are located in the center of control volumes and velocity components on cell faces. The algorithm solution of the pressure field, which is essential for the determination of the velocity field, is obtained using the SIMPLEST algorithm based on the SIMPLE algorithm. These pressure-velocity coupling algorithms is based on a sequence of prediction-correction of pressure and velocity fields until satisfaction of continuity and momentum equations (Patankar, 1980).

3- RESULTS ANALYSIS

3.1- Grids of the study domain

In a non orthogonal curvilinear grid, the grid lines follow the studied domain boundaries. A 3-D structured grid is generated to study the three-dimensional flow structures in the Laroussia dam reservoir (Figure 3). The grid number NX, NY and NZ

(respectively in the longitudinal, lateral and vertical direction) is 76x20x10 = 15200 and has for minimum grid angle : θ_{min} = 37.3°.

The study domain of the depth-averaged two-dimensional hydrodynamic model is discretized by a MB-FGE grid composed by two blocks: the first block represents the MCB intake convergent and the second represents Laroussia resrevoir (Figure 2). This decomposition of the domain allowed to overcome difficulties associated to the large dimension variations between the reservoir and the lateral MCB intake since the grid of each block is generated independently. However, the hydrodynamic field is solved simultaneously on the two blocks. This grid is more refined in the convergent and has respectively in longitudinal and lateral directions, NXxNY = 118x20 = 2360 grids with a minimal angle : θ_{min} = 38.5°. The grid number at the connexion interface between the two blocks is taken equal to 9 grids in block 2. This number is 12 in the 3-D structured grid. Velocity components at the MCB intake exit are then determined by linear interpolation from results of the 2-DH hydrodynamic model.

Another grid structure is adopted on the field scale of the Laroussia dam due to the distortion of hydraulic model (Figure 4). The generated grid has a minimal angle of 39.1° for a grid number of 76x30x10 = 22800 (respectively in the longitudinal, lateral and vertical direction).

These grids are, firstly, verified by assuming potential flows (Hafsia and Maalel, 1998). This assumption allows a much faster grid choice with minimal grid angle. In fact, computation time is relatively low compared to the case where full terms in the transport equations are considered (convection, diffusion and pressure gradients).

3.2- Mass imbalances winthin the cell

To acheive the computation convergence, it is necessary to verify that the mass imbalances (IMB1) winthin each cell satisfy the following condition :

$$IMB1 < IMB1^{*} \qquad \text{(10-a)}$$

with : $$IMB1^{*} = 10^{-3}\frac{\rho U_{in} A_{in}}{n_{in}} \qquad \text{(10-b)}$$

where, U_{in} and A_{in} are respectively the velocity and the inlet domain area. They have for values at the hydraulic model: U_{in} = 4.3 10^{-3} m/s; A_{in} = 0.305 m^2 (on the field scale, these values are divided respectively by kinematic similarity ratio, U_r = 1/5, and surfaces ratio,

A_r = 1/2500). The grid number at the inlet, n_{in}, is fixed to 20 grids on the hydraulic model scale and 30 grids on the field scale.

Based on the results summarized on table 1, we note that the condition (10) is well verified on the hydraulic model sacle as well as on the prototype. To assure the convergence of computation, a linear relaxation coefficient of the pressure equal to 0.1 was used.

Table 1 : Mass balance within cell

	Hydraulic model scale	Field scale	
IMB1* (Kg/s)	$6.5\ 10^{-5}$	2-DH : $8.0\ 10^{-1}$	3-D : $5.3\ 10^{-1}$
2-DH hydrodynamic model			
IMB1 (Kg/s)	$-1.0\ 10^{-9} \div 9.3\ 10^{-10}$	$-9.7\ 10^{-6} \div 9.7\ 10^{-6}$	
3-D hydrodynamic coupled with 2-DH model			
IMB1 (Kg/s)	$-3.0\ 10^{-8} \div 3.0\ 10^{-8}$	$-1.7\ 10^{-4} \div 2.1\ 10^{-4}$	

3.3- Comparison between the currents structures before and after approach-channel implementation

Photo 1 shows the bottom currents structure in the case of the MCB intake opening with its maximum discharge, Q = 1.3 l/s, and the water level in the Laroussia dam reservoir is fixed at its normal level, 37.50 m. These streamlines are visualized by grains of potassium permanganate. The upwelling of these currents along the length of the MCB intake crest, fixed at 34.84 m, explains the sediments entrance in the MCB channel (Photo 1-a). The numerical simulations results of the depth-averaged two-dimensional hydrodynamic model show that this model reproduce the visualized streamlines structure in the MCB intake convergent, where the depth is relatively small (Figure 5). However this model can not reproduce the bottom currents upwelling toward the intake that causes the observed deposits in the MCB channel. Hence, three-dimensional hydrodynamic model is necessary. This model is coupled with the the 2-DH model results through boundary conditions at MCB intake exit. The simulated and visualized currents structures on the hydraulic model scale allowed the developement of comparison criteria between three alternatives of training wall aiming to modify the direction of the bottom currents in order to reduce their upwelling toward the MCB intake (Hafsia and Maalel, 1999). The retained

alternative is a training wall open at its downstream extremity. By modifying the shape of the MCB entrance, this training wall was materialized by an approach-channel as illustrated by Photo 1-b. Under the effect of this approach-channel, the visualized bottom currents in the vicinity of the MCB intake show a well reduction of the currents upwelling toward this intake.

These results are confirmed by the analysis of the secondary current's structure on the profile located upstream of the MCB intake. These secondary currents are defined in a perpendicular section to the flow direction and have for intensity $V_s = \sqrt{V^2 + W^2}$ (where V and W are the averaged velocity components respectively in the lateral and vertical directions). Figure 6 shows these current's structure at profile M (the location of this profile is presented on Figure 3). Without control device, the secondary currents on the right side bank, in which the MCB intake is located, are ascending toward the MCB intake. These current's direction is inversed under the effect of the approach-channel. This inversion is expected to reduce bottom currents upwelling toward the MCB intake and threfore the entrance of muds in this intake. This currents inversion is also confirmed on field scale simulation (Figure 7). Their effect extend along a distance of about 31 m upstream of the MCB. This approach-channel also favorizes the MCB intake's alimentation by water coming from nearby the dam which is much clear due to the velocity reduction in this region.

4 - CONCLUSION

The depth avareged two-dimensional hydrodynamic model is sufficient to reproduce the visualized streamlines in the MCB intake convergent. To reproduce the upwelling of the bottom currents in front of the MCB intake, three-dimensional hydrodynamic model is used. This model is coupled to the 2D-H hydrodynamic model to take into account the effect of the MCB intake convergent on the Laroussia reservoir flow. In accordance with the visualized currents on hydraulic model, the analysis of the simulated secondary currents structures showed that an approach-channel allowed the inversion of secondary currents upstream of the MCB intake. The advantage of this proposed waterwork is also confirmed by numerical simulation on the prototype. The coupling of this hydrodynamic model to a suspended sediment transport model, in a second phase of this study, will permit to quantify the reduction of sediments quantities entering the intake under the effect of the proposed approach-channel.

REFERENCES

[1] Atkinson, E. - Performance Prediction and design Methods for canal Sediment Extractors. OD/P67 (1988).

[2] Bouvard, M. – « Barrages mobiles et ouvrages de dérivation à partir de rivières transportant des matériaux solides. Eyrolles (1984) ».

[3] Hafsia, Z. et Maalel, K. – « Simulations numériques en 3-D des écoulements au voisinage de la prise d'eau Medjerda-Cap-Bon. Choix d'une variante d'aménagement ». Septième Conférence Annuelle de la CFD. Halifax, Canada, 30 mai-1er Juin (1999).

[4] Hafsia, Z. et Maalel, K. – « Vérification des maillages BFC et MB-FGE de la retenue du barrage Laroussia et de la prise Medjerda-Cap-Bon ». 6ième Colloque Maghrébin sur les modèles numériques de l'Ingénieur (C2MNI6),Tunis. 24-26 novembre (1998). pp. 595-600.

[5] Henderson, F.M. - Open channel Flow. Macmillan (1966).

[6] Higgs, James A. - Folsom Dam Spillway Vortices Computational Fluid Dynamic Model Study. Water Resources Research Laboratory (1997). http://ogee.do.usbr.gov/jhiggs/folsom/

[7] Jian, Ye and McCorquodale, J.A. – Depth-averaged hydrodynamic model in curvilinear collocated grid. Journal of Hydraulic Engineering, Vol 123, N°5, pp380-401 (1997).

[8] Patankar, S.V. - Numerical heat transfer and fluid flow. Hemisphere Publishing Corporation (1980).

[9] Schiestel, R. – « Modélisation et simulation des écoulements turbulents ». Hermes (1993).

[10] Smith, K.M.; Cope, W.K. and Vanka, P.– A multigrid procedure for three-dimensional flows on non-orthogonal collocated grids. Int. J. for Num. Meth. in Fluids. Vol. 17, pp.887-904 (1993).

[11] Wang, S.S. Y. - Computational modelling of alluvial rivers. Computational Water Resources (1991).

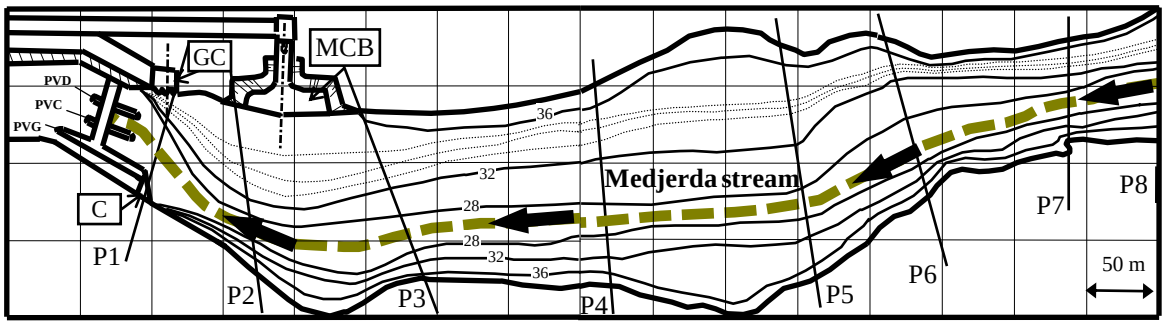

Figure 1 : Layout plan of three water intakes of the Laroussia mobile dam.

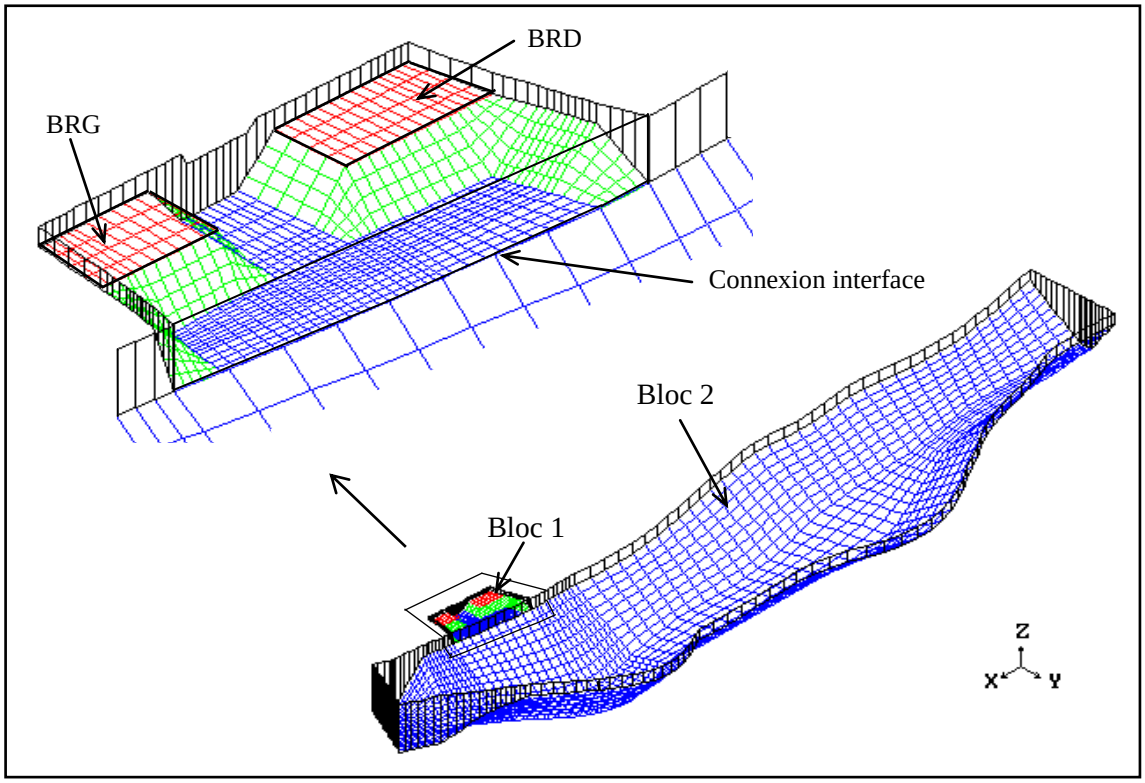

Figure 2 : Two-dimensional multiblocks grid of the Laroussia dam reservoir

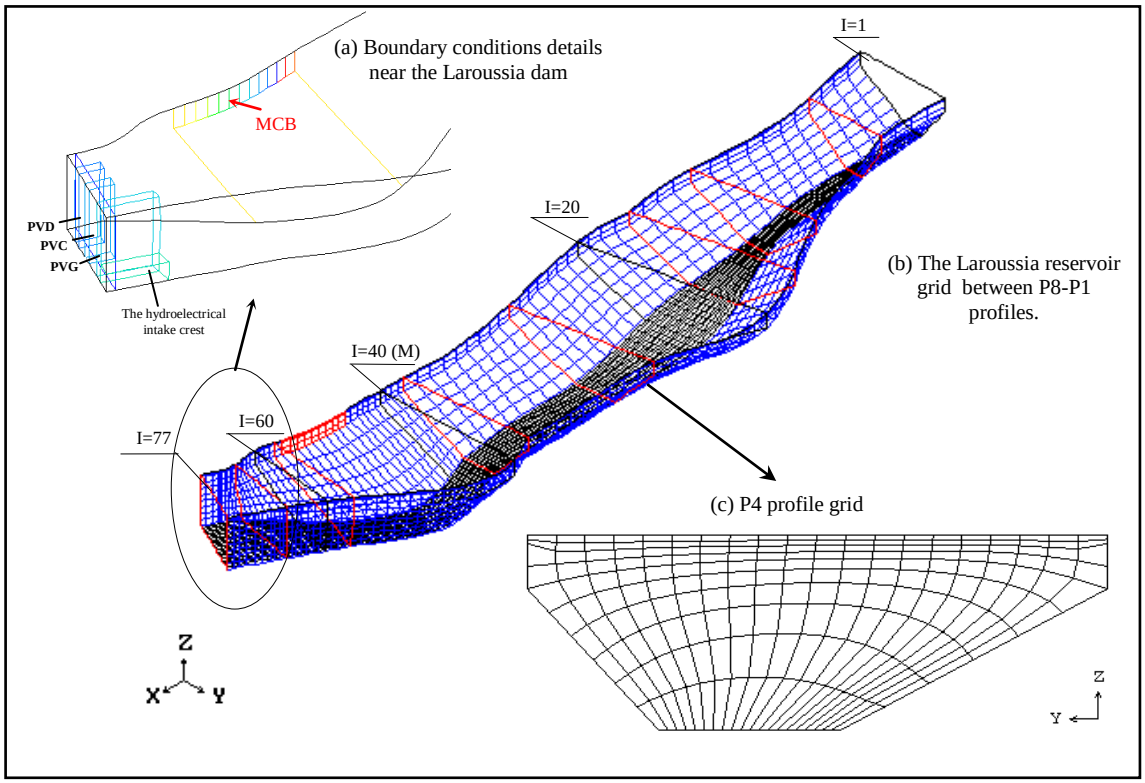

Figure 3 : Three-dimensional grid on of the Laroussia dam reservoir (on hydraulic model scale).

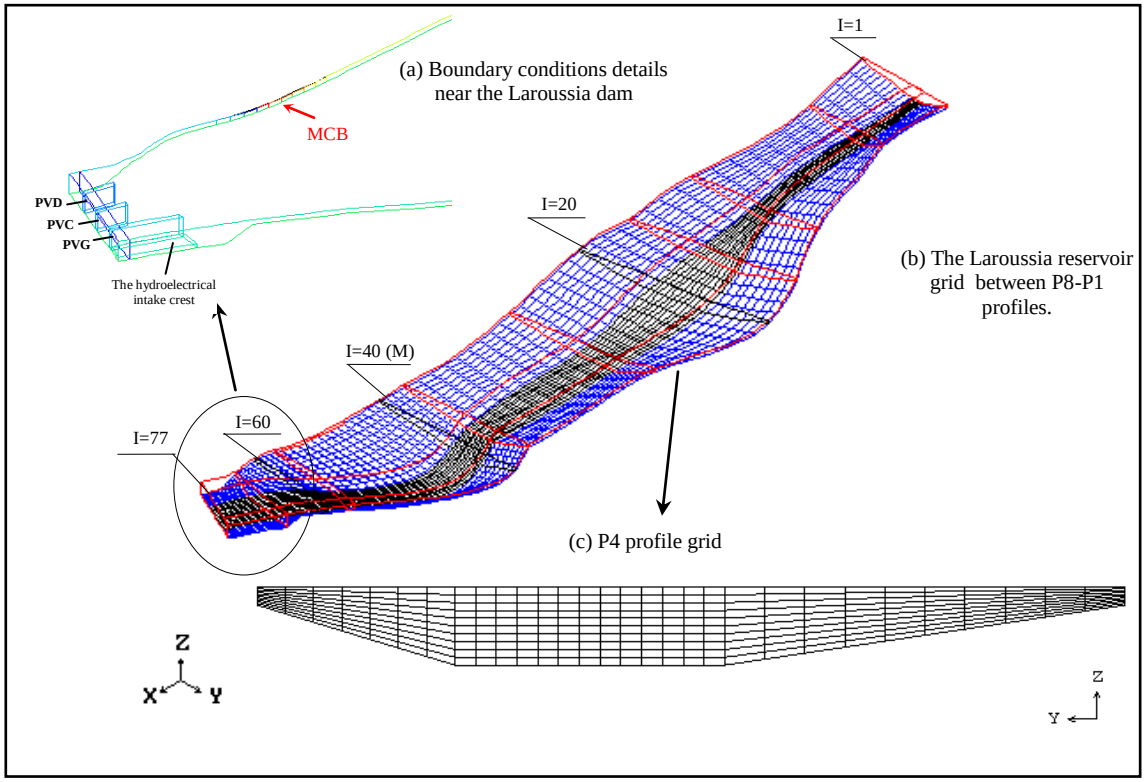

Figure 4 : Three-dimensional grid of the Laroussia dam reservoir (on field scale).

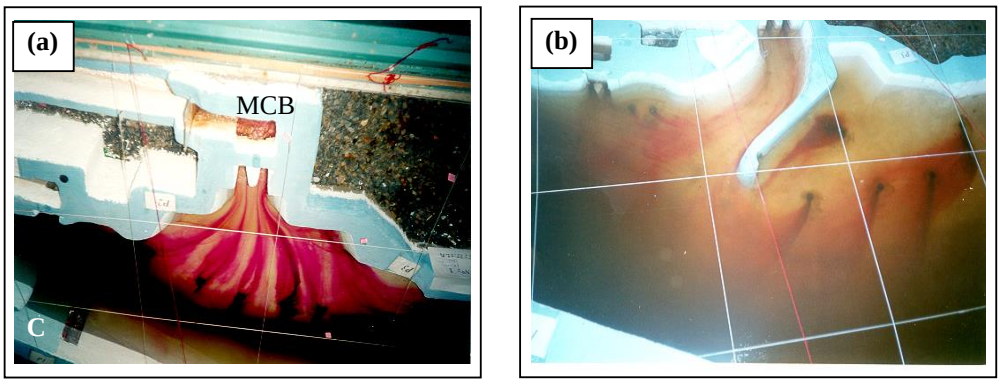

Photo 1 : Bottom currents upwelling in the vicinity of the MCB water intake visualized on the hydraulic model of the Laroussia dam (Q = 1.3 l/s).
a) Without approach-channel.
b) After approach-channel implementation.

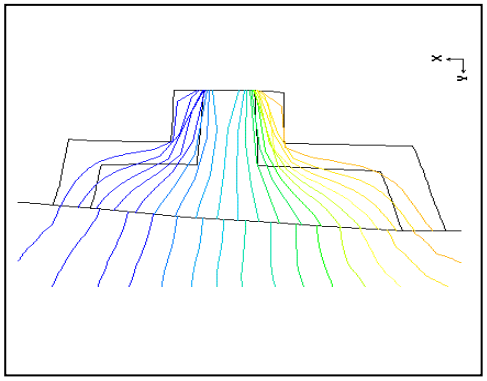

Figure 5 : Streamlines structure in the vicinity of the MCB water intake simulated by 2-DH hydrodynamic model.

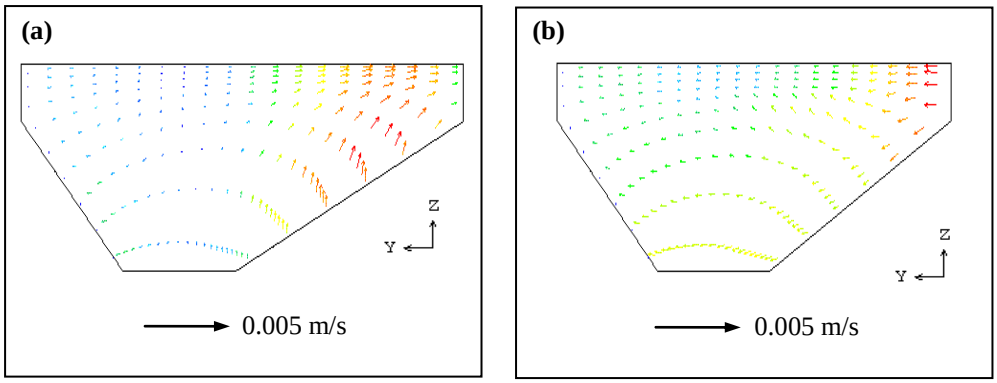

Figure 6 : Simulated secondary current's structure on the cross profile (M) upstream of the MCB intake, Q = 1.3 l/s ($\nu_t = 5\ 10^{-5}$ m^2/s).

Without approach-channel.

After approach-channel implementation.

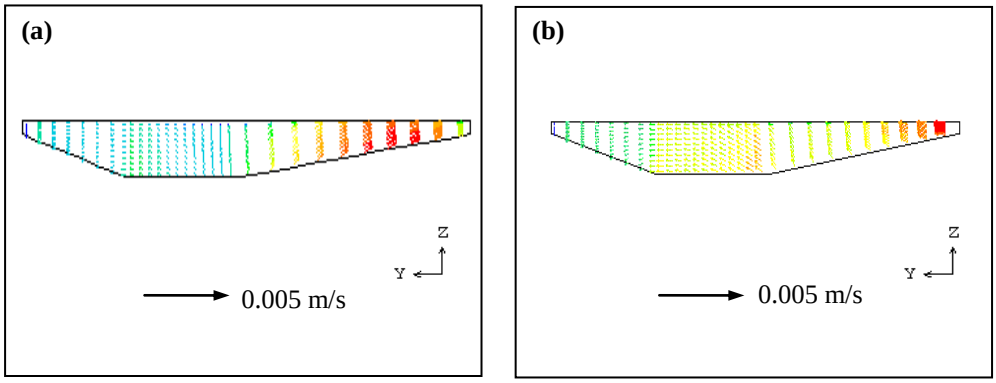

Figure 7 : Simulated secondary current's structure on the cross profile (M) upstream of the MCB intake, Q = 16 m^3/s ($\nu_t = 2.5\ 10^{-2}$ m^2/s).

a) Without approach-channel.

b) After approach-channel implementation.